J Fluoresc (2010) 20:353–364
DOI 10.1007/s10895-009-0564-x

ORIGINAL PAPER

Efficiently Tuning the Absorption and Fluorescence Spectroscopy of the Novel Branched p-Nitro-stilbene Derivatives with Chemical Strategy

Fang Gao · Liufeng Yang · Long Yang · Hongru Li · Shengtao Zhang

Received: 15 September 2009 / Accepted: 3 November 2009 / Published online: 2 December 2009

Abstract Suitable chemical strategy is a useful approach on the tuning color and photoluminescence of organic dyes. This paper presented tuning novel branched p-nitro-stilbene derivatives efficiently with a new chemical strategy through variation of chemical bridged bond. Linking bonds played significant effects on the absorption and fluorescence spectroscopy of the branched p-nitro-stilbene derivatives. A change from "D-π-A" to "A-π-A" chemical structural characteristics occurred for the branched p-nitro-stilbene derivatives as ester bond was attached. This led to not only large hypsochromic shift of the maximal absorption wavelength of the branched p-nitro-stilbene derivatives, but considerable reduction of the fluorescence intensity. While in contrast, the branched p-nitro-stilbene derivatives with ether bond exhibited longer wavelength absorption and much stronger fluorescence emission in modest polar solvent. The cyclic voltammograms of these branched p-nitro-stilbene derivatives were determined. Different electrochemistry processes were observed for the branched p-nitro-stilbene derivatives with various linking bonds. The energies of frontier orbital of the branched p-nitro-stilbene derivatives were estimated from their corresponding redox potentials. Molecular geometry optimization of the branched p-nitro-stilbene derivatives was performed, and the electron density distribution of frontier orbital was analyzed. Thermal stabilities of these branched nitro-stilbene derivatives were investigated via the analysis of the differential scanning calorimetry (DSC) and thermograving (TGA) curves. This paper presented strong evidences that the absorption and fluorescence spectroscopy of the branched stilbene derivatives could be mediated efficiently by chemical strategy.

Keywords Stilbene derivatives · Branched compound · Synthesis · Spectroscopy · Molecular geometry optimization · Electrochemistry · Chemical strategy

F. Gao (✉) · L. Yang · L. Yang · H. Li · S. Zhang
College of Chemistry and Chemical Engineering,
Chongqing University,
Chongqing 400044, China
e-mail: fanggao1971@gmail.com

Introduction

During the past years, organic dyes have been investigated extensively due to their broad applications such as in biomedical, photoelectronic material, and three-dimensional micro-device fabrication, and they offer many advantages such as easy fabrication and reducing production costs [1–6]. In looking for high quality organic dyes with ideal spectroscopic nature, the chemical structures of the dyes have been shown to a strong relationship with their spectral characteristics [7]. Hence, the investigation of the effects of chemical structures on the absorption and emission spectroscopic properties of organic dyes becomes one of significantly important research areas in photochemistry and photophysics. Gratzel et al demonstrated that tuning the frontier orbital of organic dyes by various substituent groups was very useful strategy for the fabrication of high efficient dye-sensitized solar cells [8, 9]. It is well accepted that substituent groups not only can alter the extent of intramolecular charge transfer, but the properties of excited state properties, which is achieved by the variation of the energy and the electron density distribution of frontier orbital [10, 11].

Stilbene-like dye is one of the most important classes of dyes, which has received considerable attention as organic materials for optical power limiting and electrooptical

devices [12, 13]. The polarizablility and second hyperpolarizabilities of these molecules tightly depends on molecular structures of stilbene derivatives, thus enormous efforts have been devoted on the development of stilbene derivatives with various structural features such as donor-π-acceptor and donor-π-donor [14–16]. Some studies have been concentration on the enlarging absorption wavelength and enhancement of fluorescence emission of stilbene derivatives [17, 18]. The photophysical properties of several selectively bridged stilbenes with donor-acceptor substituent groups of various were investigated [19]. While to date, few comparable investigations on development of new stilbene derivatives with various spectral characteristics of blue-shifted or red-shifted UV/visible absorption spectroscopy and strong or weak fluorescence emission have been reported. This paper presented some novel branched nitro-stilbene derivatives, of which particular interest is if we could tune successfully the absorption wavelength and fluorescence emission via new chemical strategy. Various linking chemical bonds were proposed to tune color and photoluminescence of nitro-stilbene derivatives. Molecular geometry optimization and electrochemistry of these dyes were carried out to further understand interrelationship of the chemical structures and absorption and fluorescence spectroscopy. The thermal stabilities of the compounds were determined and analyzed.

Experimental

Materials

The chemicals and reagents were purchased from Chongqing Medical and Chemical Corporation unless otherwise specified. The organic solvents were dried using standard laboratory techniques according to published methods [20]. The starting materials were further purified via reinstallation or recrystallization before use. **C1**, **C2**, **C3** and **C4** were synthesized in our laboratory and their chemical structures were shown in Fig. 1.

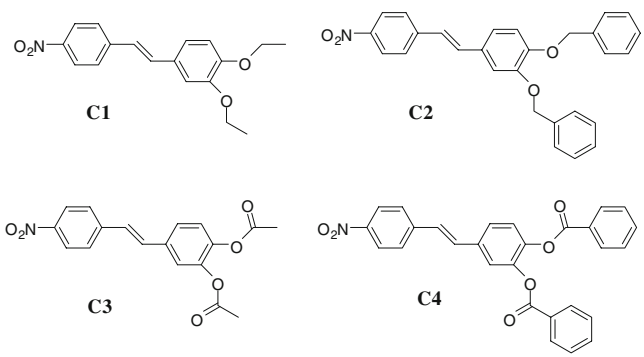

Fig. 1 Chemical Structures of Nitro-Stilbene Derivatives

Instruments

The UV/visible absorption spectra were recorded with a Cintra spectrophotometer. The emission spectra were checked with Shimadzu RF-531PC spectrofluorophotonmeter. Quinine sulfate in 0.5 M H_2SO_4 (Φ=0.546, 1×10^{-6}-$\times10^{-5}$mol/L [21]) was used as a reference to determine the fluorescence quantum yields of the compounds in this study. The melting point was determined using an uncorrected Beijing Fukai melting point apparatus. Nuclear Magnetic Resonance (NMR) was carried out at room temperature with a Bruker 500 MHz apparatus with tetramethylsilane (TMS) as internal standard and $CDCl_3$ was used as solvent. Element analysis was detected by CE440 elemental analysis meter from Exeter Analytical Inc.

The fluorescence quantum yields of the compounds in various solvents were determined based on the following equation [22, 23]:

$$\Phi_f = \Phi_f^0 \frac{n_0^2 A \int I_f(\lambda_f) d\lambda_f}{n^2 A \int I_f^0(\lambda_f) d\lambda_f} \quad (1)$$

Wherein n_0 and n are the refractive indices of the solvents, A^0 and A are the absorption at excited wavelength, Φ_f and Φ_f^0 are the quantum yields, and the integrals denote the area of the fluorescence bands for the reference and sample, respectively.

The time-resolved fluorescence curves were determined on an Edinburgh FLS920 time-correlated single photon counting unit. The lifetimes were calculated from decay curves using the least-squares method.

Molecular structure optimization calculations

Structure optimization was performed with the HyperChem 8.0 package [24] choosing the with AM1 semiempirical quantum chemical method [25] to keep computations tractable.

Electrochemistry

Electrochemical measurements were carried out using a Shanghai Chenhua working station. Two Pt work electrodes and an Ag/Ag^+ reference electrode, i.e. three electrodes system, were included in cell. Typically, a 0.05 mol/L solution of tetra-n-butylammonium hexaflorophosphate in CH_2Cl_2 containing of sample was bubbled with argon for 15 min. The scan rate was 0.1 V/s.

Thermal analysis

The differential thermal analysis (DTA) and thermogravimetric analysis (TGA) were conducted under nitrogen gas

flow in Shimadzu DTG-60H equipment at heating rate 10°C min^{-1}.

Synthesis of nitro-stilbene derivatives

Synthesis strategies of **C1** to **C4** were shown in Scheme 1. p-Nitro-3',4'-dihydroxyl-stilbene was prepared according to published method [26].

C1 (3, 4-diethoxy-4'-nitrostilbene) **C1** was prepared as followings. (2.0 g, 7.8 mmol) p-Nitro-3', 4'-dihydroxyl-stilbene and bromoethane (2.5 g, 23.4 mmol) was dissolved in 100 ml dried acetone, Anhydrous potassium carbonate (4.3 g, 31.2 mmol) and a few 18-C-6 were added to the solution. The reactant mixture was stirred at room temperature under argon for 24 hr. The solid was got rid of solution by filtration and THF was removed fully by evaporation. The resulting mixture was dissolved in $CHCl_3$ and washed by water for three times. The organic layer was dried with anhydrous sodium sulfate and then concentrated. The product was purified by column chromatography. Further purification was carried out with twice recrystallization from benzene to yield 0.95 g (3.0 mmol) salmon pink of **C1** (yield 39 %).^{1}H-NMR (δ: ppm): 8.19 (d, J= 9.0 Hz, 2H, CC*H*CH), 7.58 (d, J=8.5 Hz, 2H,CHC*H*C), 7.16 (d, J=16.0 Hz, 2H, CC*H*CH), 7.0 (d, J=7.5 Hz, 2H, CC*H*CH), 6.84 (d, J=8.5 Hz, 1H, CHC*H*C), 4.16 (m, J= 7.0 Hz, 4H, OCH_2CH_3), 1.47 (t, J=7.0 Hz, 6H, CH_2CH_3). ^{13}C-NMR(δ: ppm), 14.830, 64.626, 111.467, 112.032, 120.258, 124.138, 126.570, 129.771, 133.048, 144.207, 146.039, 146.458, 146.658. Melting point: 152–153.5°C. Anal. calculated, C, 68.99, H, 6.11, N, 4.46, O, 20.42, Found, C, 68.11, H, 5.92, N, 4.51.

C2 (3, 4-dibenzyloxy-4'-nitrostilbene) **C2** was prepared as followings. (2.0 g, 7.8 mmol) p-Nitro-3', 4'-dihydroxyl-stilbene and benyl bromide (4.0 g, 23.4 mmol) were dissolved in 150 ml dried acetone, Anhydrous potassium carbonate (4.3 g, 31.2 mmol) and a few 18-C-6 were added to the solution. The reactant mixture was stirred at room temperature under argon for 24 hr. The solid was got rid of solution by filtration and THF was removed fully by evaporation. The resulting mixture was dissolved in $CHCl_3$ and washed by water for three times. The organic layer was dried with anhydrous sodium sulfate and then concentrated. The product was purified by column chromatography. Further purification was carried out with twice recrystallization from benzene to yield 1.6 g (3.6 mmol) golden yellow of **C2** (yield 46%). ^{1}H-NMR (δ: ppm): 8.19 (d, J= 9.0 Hz, 2H, CC*H*CH), 7.57 (d, J=9.0 Hz, 2H, CHC*H*C), 7.48 (dd, J=7.5 Hz, 4H, CC*H*CH), 7.39 (dd, J=7.5 Hz, CHC*H*CH), 7.33 (t, J=2.8 Hz, 2H, CHC*H*CH), 7.15 (d, J= 17.5 Hz, 2H, CC*H*CH), 7.08 (d, J=9.5 Hz, 1H, CHC*H*C), 6.95(d, J=6.5 Hz, 2H, CC*H*CH), 5.22 (s, 4H, OCH_2C). ^{13}C-NMR(δ: ppm):71.119, 113.216, 114.718, 121.394, 124.128, 126.594, 127.234, 127.352, 127.954, 128.558, 129.856, 136.922, 144.083, 146.468, 149.135, 149.915. Melting point:136.5–137°C. Anal. Calculated, C, 76.87, H. 5.30, N, 3.20, O, 14.63, Found, C, 76.10, H, 5.38, N, 3.31.

C3: (3, 4-diacetoxy-4'-nitrostilbene) **C3** was prepared as followings: p-Nitro-3',4'-dihydroxyl-stilbene (1.5 g, 5.8 mmol) and triethylamine (TEA) (4.6 g, 4.64 mmol) was dissolved in dry THF. Acetic anhydride (3.5 g, 34.8 mmol) was dropped slowly. The mixture was stirred at room temperature under argon for 24 hr. The solid was got rid of solution by filtration and the solvents were removed fully by evaporation. The resulting mixture was dissolved in $CHCl_3$ and washed by water for three times. The organic layer was dried with anhydrous sodium sulfate and then concentrated. The product was purified by column chromatography. Further purification was carried out with twice recrystallization from benzene to yield 0.84 g (2.5 mmol) deep yellow color of **C3** (yield 42%).^{1}H-NMR ($CDCl_3$, δppm): 8.19 (d, J=8.0 Hz, 2H, CC*H*CH), 7.58 (d, J=8.0 Hz, 2H, CHC*H*C), 7.38 (d, J=9.5 Hz, 2H, CC*H*CH), 7.18 (m, J= 9.5 Hz, 2H, CHC*H*C), 7.05(d, J=18.0 Hz, 1H, CC*H*CH), 2.31 (s, 6H, CCH_3). ^{13}C-NMR, δppm: 20.657, 121.540, 124.158, 127.460, 131.408, 135.167, 142.272, 142.437, 143.303, 146.964, 168.212. Melting point: 160–161.5°C. Anal. Calculated, C, 63.34, H, 4.43, N, 4.10, O, 28.13, Found, C, 63.90, H, 4.36, N, 3.86.

C4: (3, 4-dibenzoyloxy-4'-nitrostilbene) The title compound was prepared as followings: p-Nitro-3', 4'-dihydroxyl-stilbene (1.5 g,5.8 mmol) and triethylamine (TEA) (4.6 g, 46.4 mmol) was dissolved in dry THF. Benzoyl chloride (4.9 g, 34.8 mmol) was dropped slowly. The mixture was stirred at room temperature under argon for 24 hr. The solid was got rid of solution by filtration and the solvents were removed fully by evaporation. The resulting mixture was dissolved in $CHCl_3$ and washed by water for three times. The organic layer was dried with anhydrous sodium sulfate and then concentrated. The product was purified by column chromatography. Further purification was carried out with twice recrystallization from benzene to yield

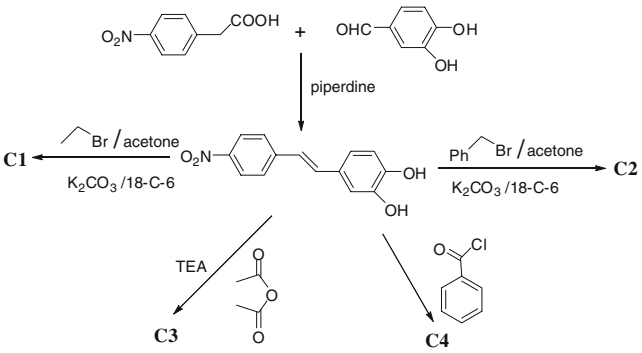

Scheme 1 Synthesis route of branched nitro-stilbene derivatives

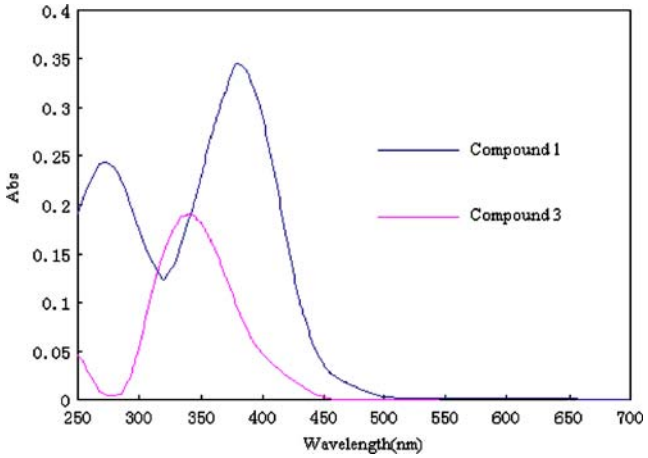

Fig. 2 Typical comparison of absorption spectroscopy of C**1** and C**3** in methylene chloride (1×10^{-5}mol/L)

1.1 g (2.3 mmol) light yellow color of **C4** (yield 40%). ^{1}H-NMR δ(ppm): 8.19 (d, J=9.0 Hz, 2H, CC*H*CH), 7.57 (d, J=9.0 Hz, 2H, CHC*H*C), 7.48 (dd, J=7.5 Hz, 4H, CC*H*CH), 7.39 (dd, J=7.5 Hz, CHC*H*CH),7.33 (t, J=2.8 Hz, 2H, CHC*H*CH), 7.15 (d, J=17.5 Hz, 2H, CC*H*CH), 7.08 (d, J=9.5 Hz, 1H, CHC*H*C), 6.95 (d, J=6.5 Hz, 2H, CC*H*CH), 5.22 (s, 4H, OCH_2C). ^{13}C-NMR(δ: ppm): 121.637, 123.951, 124.187, 127.494, 128.562, 128.621, 130.188, 131.562, 133.816, 142.768, 142.962, 143.357, 146.971, 164.242. Melting point: 153–154.5°C. Anal. Calculated, C, 72.25, H, 4.11, N, 3.01, O, 20.62, Found, C, 71.67, H, 4.16, N, 3.26.

Results and discussion

Spectroscopic properties

The UV-visible spectroscopy

C1 and **C2** exhibited remarkably different absorption characterization from **C3** and **C4**. Typical ultraviolet/visible absorption spectroscopy of **C1** and **C3** in methylene chloride was shown in Fig. 2. Clearly, the maximal absorption wavelength of **C3** exhibited considerable blue-shift with respect to that of **C1** in methylene chloride. The data shown in Table 1 suggested clearly: (1) the maximal absorption wavelength of **C1** and **C2** underwent evident bathochromic shift in polar solvents (*ca.* 15 nm); while as sharp contrast, **C3** and **C4** featured with tiny red-shift (*ca.* 4 nm). This is an indication that polar solvents and ether bond could stabilize the intramolecular charge transfer states of **C1** and **C2**, while the intramolecular charge transfer states of **C3** and **C4** could be destabilized by polar solvents and ester bond [27, 28]. (2) Nitro-stilbene derivatives with ester bridged bonds displayed *ca.* 30–40 nm blue-shift on the maximal absorption wavelength with respect to nitro-stilbene derivatives with ether bridged in various solvents. This caused remarkably different color of **C1** and **C2** from **C3** and **C4** as shown in Fig. 3. This suggested that the intramolecular linking bonds had significant effects on the absorption spectroscopy of the nitro-stilbene derivatives. It was mostly due to the effects of linking bond on the extent of intramolecular charge transfer. The ultraviolet/visible absorption characteristics of **C1** and **C2** indicated a highly allowed π-π* electron transition with strong intramoclecular charge transfer feature [29, 30], while the low optical density and the blue-shifted wavlength implied that the absorption of **C3** and **C4** could be ascribed to prohibited n-π* electron transition nature [31]. The extent of intramolecular charge transfer of **C1** and **C2** could be diminished by the electron deficiency effect of ester bridged bond. While, ether linking bond could increase the extent of intramolecular charge transfer due to its electron-donating effect. The chemical structural characteristics of **C3** and **C4** exhibited great change from donor-π-acceptor to acceptor-π-acceptor as the introduction of the ester bond, which could lead to the reduction in the intramolecular charge transfer of **C3** and **C4**. Typical comparison of the sketch of molecular structures of **C2** and **C4** was shown in Fig. 4. Hence, the π-π* electron transition of **C1** and **C2** was strengthened, and the n-π* electron transition of **C3** and **C4** was further inhibited.

Table 1 Experimental absorption spectral data of **C1** to **4** in various solvents

Solvents	$\lambda_{a,max}$ (nm)				ε (1×10^5) L/mol·cm			
	C1	C2	C3	C4	C1	C2	C3	C4
Cyclohexane	357	360	333	335	0.134	0.121	0.105	0.0894
Benzene	379	375	337	341	0.118	0.114	0.108	0.109
Ethyl acetate	375	374	334	337	0.215	0.189	0.146	0.101
THF	383	381	338	337	0.336	0.200	0.111	0.117
CH_2Cl_2	381	381	339	341	0.344	0.273	0.189	0.149
CH_3CN	379	379	338	342	0.251	0.358	0.102	0.108

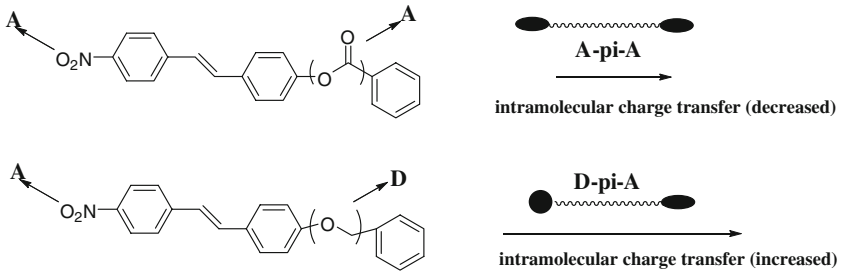

Fig. 3 Colors of C1 to C4 in THF solvent

These could result in blue-shift of the maximal absorption wavelength of nitro-stilbene derivatives with ester linking bonds. Thus, this is possible to tune the absorption spectroscopy of nitro-stilbene derivatives by various chemical linking bonds.

The fluorescence spectroscopy

C1 and **C2** featured with strong emission in modest polar solvents. While in sharp contrast, **C3** and **C4** exhibited exceptional weak fluorescence emission in various solvents. A typical comparison of fluorescence spectroscopy of **C1** and **C3** in methylene chloride was shown in Fig. 5. The results showed that linking bond played significant effect on the fluorescence spectroscopy of nitro-stilbene derivatives as well. This implied that the excited state properties of these compounds were different.

The fluorescence emission of **C1** and **C2** could be ascribed to $\pi^* \rightarrow \pi$ excited state decay. In contrast, the fluorescence emission of **C3** and **C4** could be from $\pi^* \rightarrow$n excited state decay. It is well accepted that (n, π^*) electron transition is typical forbidden transition [32], while (π, π^*) electron transition is allowed transition [33]. As discussed, the change from donor-π-acceptor to acceptor-π-acceptor occurred as ester linking bond was introduced and the electron density distribution of stilbene part of **C3** and **C4** was assumed to be diminished. While in contrast, the electron density distribution nitro-stilbene part of **C1** and **C2** could be raised by ether bridged bond. These could cause further decreasing (n, π^*) electron transition of **C3** and **C4** and further increasing (π, π^*) electron transition of **C1** and **C2** [34]. The results showed the significant effects of various linking bonds on the (π, π^*) and (n, π^*) electron transitions of the compounds. As a result, the fluorescence emission of **C3** and **C4** was considerably reduced. While the fluorescence emission of **C1** and **C2** was enhanced and it displayed remarkable red-shift with the increasing of solvent polarity. The difference on the fluorescence quantum yields of these compounds was shown clearly shown in Table 2.

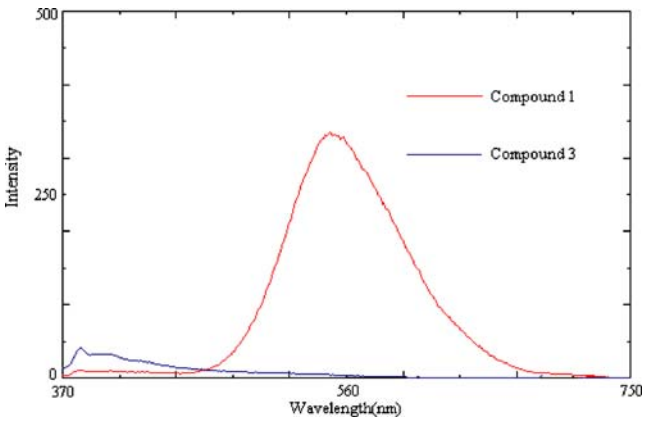

Fig. 4 A sketch of chemical structural characteristics of **C2** and **C4**

On the other hand, we observed that the fluorescence quantum yields of **C1** and **C2** was much reduced in very strong polar solvents such as acetonitrile. The variation of the fluorescence quantum yields (Table 2) of **C1** and **C2** in various solvents suggested that there existed two mechanisms dominating the decay of the excited singlet state of **C1** and **C2** [35, 36]. One was called as "negative solvatokinetic effect", which meant decreasing in the fluorescence quantum yields with suitable enhancement of intramolecular charge transfer. In other words, in non-polar solvents, the radiative transition decay of the excited state played significant role. The other mechanism was "positive solvatokinetic effect", which suggested that fluorescence quantum yields were much reduced by the strong intramolecular charge transfer for the larger polarity of solvents. We supposed that the twisted intramolecular chare transfer state of **C1** and **C2** could be formed in strong polar solvents and the fluorescence emission was thus quenched.

The fluorescence lifetimes

Because the fluorescence emission of **C3** and **C4** was extremely weak, only the fluorescence lifetimes of **C1** and **C2** could be determined. Typical time-resolved fluorescence decay curves of **C1** and **C2** in methylene chloride were presented in Fig. 6, which showed a little different decay shape. This indicated that the methoxy and benzyloxy groups had influences on the fluorescence lifetimes of nitro-stilbene derivatives, as shown in Table 3. The

Table 2 Fluorescence quantum yields of compounds **1** to **4** in various solvents

Solvent	$\lambda_{f,max}$ (nm)				Fluorescence quantum yields			
	C1	C2	C3	C4	C1	C2	C3	C4
Cyclohexane	428	427	428	428	0.0054	0.0084	0.0078	0.0069
Benzene	485	494	394	395	0.024	0.062	0.0029	0.0070
Ethyl acetate	533	531	392	392	0.18	0.29	0.0068	0.024
THF	537	531	392	392	0.13	0.39	0.034	0.053
CH_2Cl_2	549	560	403	413	0.13	0.15	0.0022	0.0094
CH_3CN	548	560	393	393	0.0009	0.0047	0.0036	0.0052

the error within 10%, five times measurements

radiative transition constants and non-radiative transition constants of the compounds **1** to **2** were calculated according to the following equations:

$$Kr = \frac{\Phi_F}{\tau} \quad (2)$$

$$Knr = \frac{1 - \Phi_F}{\tau} \quad (3)$$

wherein Φ_F is fluorescence quantum yield, τ represents as fluorescence lifetime, K_r is radiative transition constant, K_{nr} is non-radiative transition constant.

Seen from Table 3, the radiative transition constant of **C2** was larger, while non-radiative transition constant of **C2** was lower. This interpreted why the fluorescence quantum yields of **C2** were bigger than **C1**, as shown in Table 2. Stiffer structure and stronger electron-donating effects of benzyloxy groups could make the fluorescence emission of **C2** enhanced. Interesting, the fluorescence lifetimes of **C1** and **C2** was longer than that of simple stilbene (τ, 0.075 ns) [37]. It was well demonstrated that for a simple stilbene, "cis-trans" isomerization was the only approach of deactivation of the excited singlet states [38]. In the present study, intramolecular charge transfer and twisted intramolecular charge transfer states could dominate the deactivative process of the excited singlet states of **C1** and **C2** rather than only "cis-trans" isomerization due to their "D-π-A" nature, and the fluorescence lifetimes of **C1** and **C2** were thus enlarged.

Electrochemistry

The cyclic voltammograms of the **C1** to **C4** were recorded in methyl chloride from 50mVs^{-1} to 150mVs^{-1}. The results were presented in Fig. 7. Obviously, four compounds displayed different redox curves, although all of the compounds were characterized with irreversible redox processes. No pair peaks were found for all compounds, and the redox processes of all compounds were dominated by diffusion-controlled electron transfer reactions resulting from linear increasing of peak currents with the square root of scan rates.

C1 showed three reduction peaks under all sweeping rates at the negative region at 100 mV/s scan rate: −0.088 V, −0.640 V, −1.653 V. Three oxidation peaks: −0.266, −1.355, 1.237 V and were recorded for **C1.** The cyclic voltammetry of **C2** exhibited one reduction and one oxidation peaks at 100 mV/s sweeping rate. The reduction peak was got at the negative region: −0.788 V, and the oxidation peak was found at positive region: 1.087 V. Figure 7(c) shows typical cyclic voltammograms of **C3** at

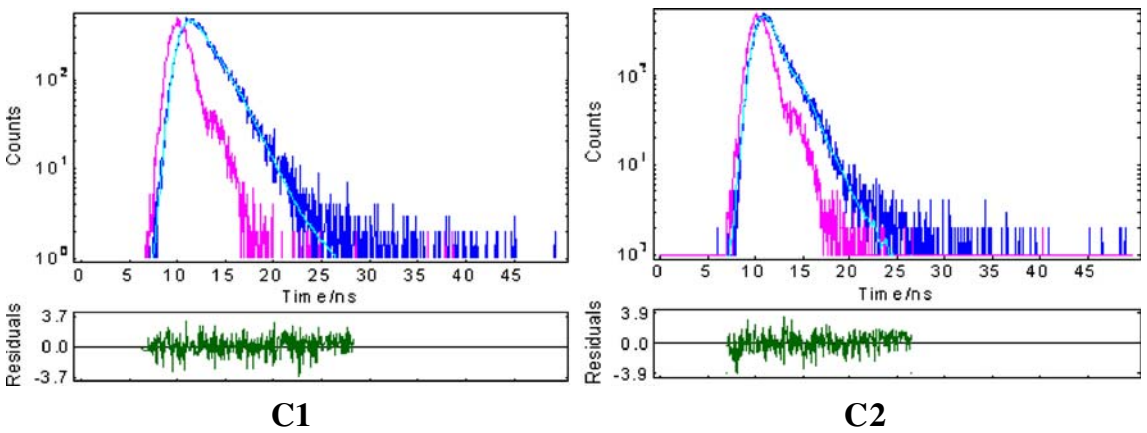

Fig. 5 Typical comparison of fluorescence spectroscopy of compounds **1** and **3** in methylene chloride (1×10^{-6}mol/L), Ex: 350 nm, Slit window: Ex: 5 nm. Em: 3 nm

Table 3 Fluorescence lifetimes, radiative transition constant, non-radiative transition constant of **C1** and **C2** in various solvents

Solvents	C1			C2		
	τ	K_r	K_{nr}	τ	K_r	K_{nr}
THF	1.93	0.674	4.508	3.03	1.287	2.013
AcOEt	1.21	1.488	6.777	2.16	1.343	3.287
CH_2Cl_2	1.81	0.718	4.807	1.73	0.867	4.913

τ: ns, K_r, K_{nr}: 10^8 /s

various scan rates. Three reduction peaks at −0.187, −0.937, 0.609 V and one oxidation peak at −0.079 V were observed at scan rate 100mVs^{-1}. Typical cyclic voltammogram of **C4** at different scan rates was shown in Fig. 7(d). Three reduction peaks were found as 0.374, −0.498, −1.273 **V**, and three oxidation peaks were observed −0.535 V, −0.094 V and 0.878 V at scan rate 100 mV/s.

Nitro group is a powerful electron-withdrawing species in **C1** to **C4** and the occurrence of its reduction reaction could be easily observed [38]. −0.640, −0.788, −0.937, −1.273 V could be regarded as reductive potentials of nitro group of **C1**, **C2**, **C3** and **C4** respectively. This showed that as compared with **C1** and **C2**, the reduction of nitro group of **C3** and **C4** became more difficult. This could be ascribed to the effect of electron-withdrawing or electron-donating of various linking chemical bonds on the redox process of nitro group. Likewise, ester bond in **C3** and **C4** as an electron-withdrawing group could undergo reduction process as well [39]. 0.609, 0.374 V could be from the reduction process of ester group of **C3** and **C4**. Furthermore, as discussed, the electron density distribution of C-C double bond could be decreased by electron-withdrawing of ester bond, and could be enhanced electron-donating effect of ether bond. This could lead to easy or difficult occurrence of redox processes on C-C double bond for these compounds respectively [40, 41], and it could be the main reason why different redox processes of these compounds were detected. The different electrochemical process reflected the difference on their HOMO and LUMO energies of these compounds [42]. Hence, we further estimated the energy of frontier orbital based on the

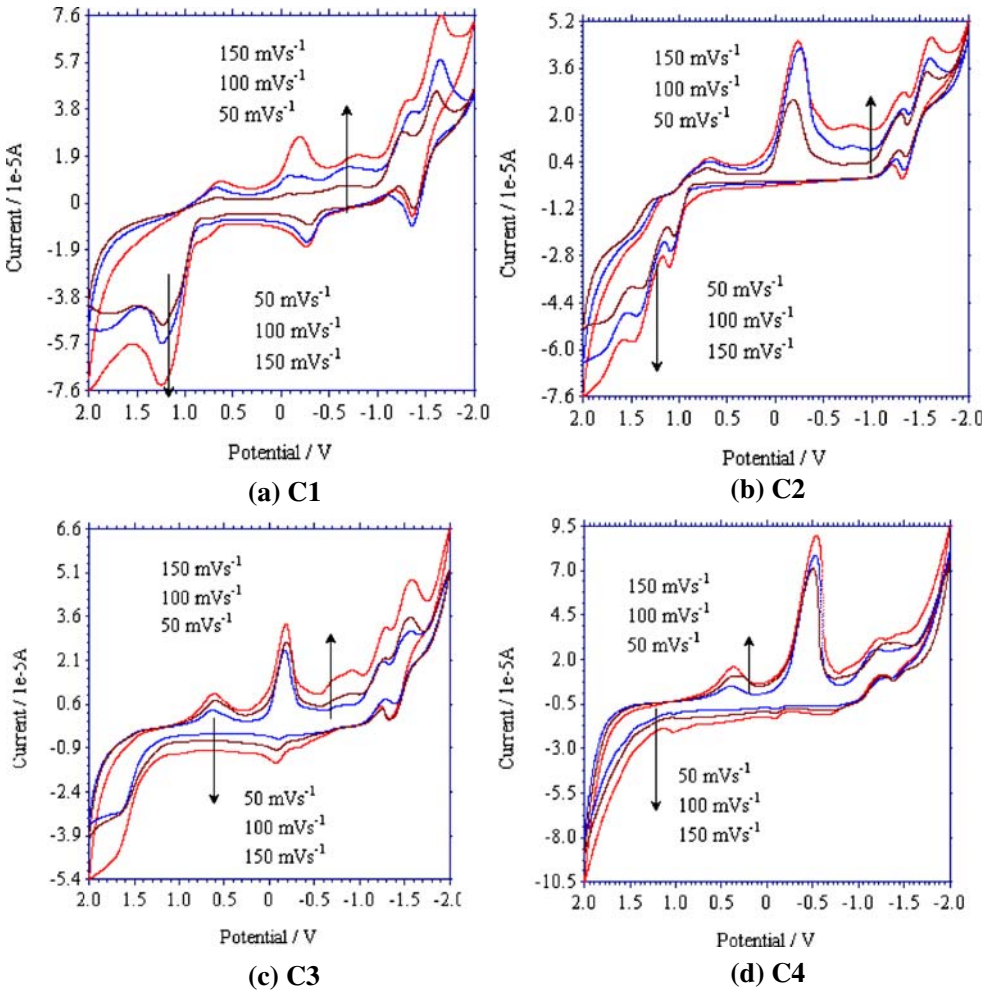

Fig. 6 Fluorescence lifetime of **C1** and **C2** in CH_2Cl_2

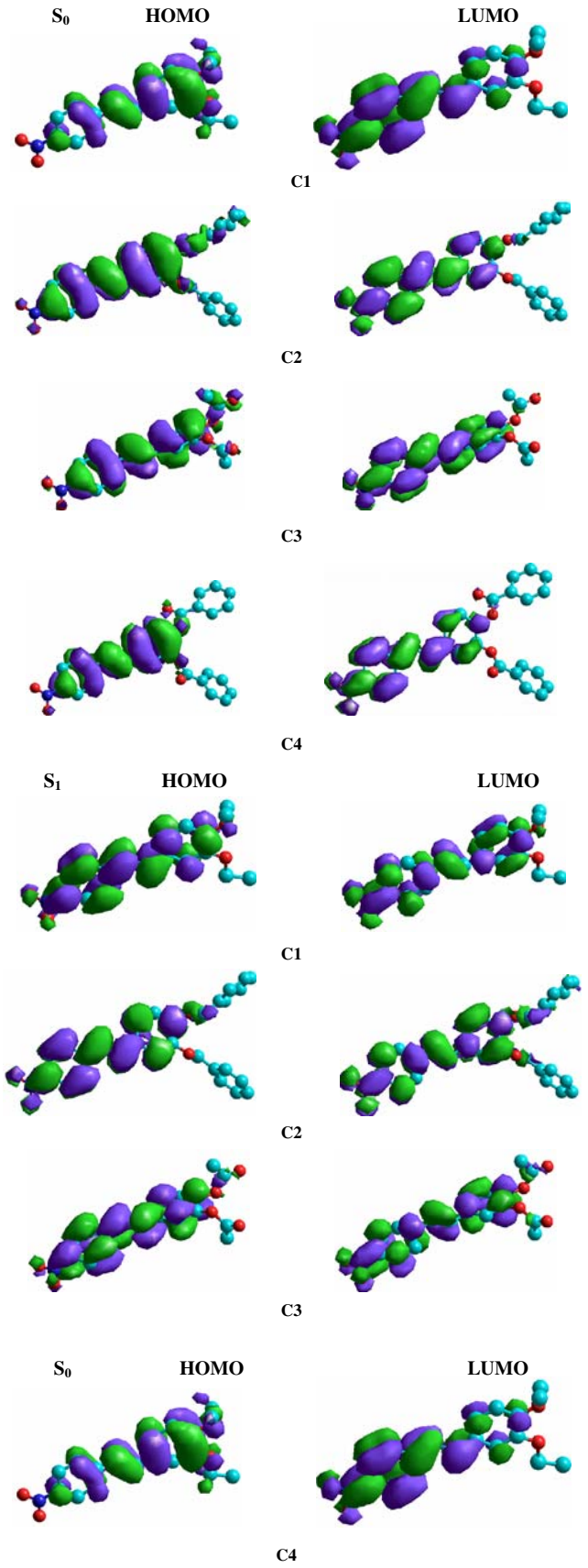

Fig. 7 Cyclic voltammograms of compounds **1** to **4** in various scan rates

corresponding redox potentials and optical parameters. The results were listed in Table 4. It clearly showed that the energy of HOMO and LUMO was enhanced by ester linking bond.

Molecular geometry optimization

The electron density distribution of HOMO and LUMO orbitals of **C1** to **C4** at S_0 and S_1 states was investigated. As shown in Fig. 8, the changes on the electron density distribution of these compounds from HOMO to LUMO transition exhibited some difference. The electron density distribution moved to nitro group and its connecting diphenyl ethylene parts in HOMO→LUMO transition at S_0 state. While as compared with **C3** and **C4**, electron density distribution of **C1** and **C2** was much closer to the side of nitro group. Electron density distribution of **C3** and **C4** exhibited more delocalization due to the deficiency effect of ester chemical bond at LUMO orbital of S_0 state. At the S_1 state, the change on the electron density distribution of **C1** and **C2** from HOMO to LUMO transition was quite different from that of **C3** and **C4**. **C1** and **C2** showed a similar change as S_0 state. However, **C3** and **C4** showed larger change on the electron density distribution from HOMO to LUMO in S_1 state. Considerable electron density distribution was found in the ester chemical linking bonds in the LUMO orbitals of **C3** and **C4** in S_1 state, especially for the ester chemical bond of **C4**. This confirmed our assumption that the electron density distribution of stilbene part of **C1** and **C2** was enhanced greatly by ether chemical bond due to the electron-donating effect. While as sharp contrast, the electron density distribution of stilbene part of **C3** and **C4** was much decreased by the electron-withdrawing effect of ester chemical bond. We further calculated the dipole moment change of these compounds between the excited state and the ground state and listed in Table 5. Obviously, **C1** and **C2** had larger dipole moment change than **C3** and **C4**. In a word, the molecular geometry optimization calculations demonstrated ester linking bond played two significant

Table 4 The estimated energy of HOMO and LUMO from Redox potentials

Compounds	E^{OX} (V)	HOMO (eV)	λonset (nm)	Gap (eV)	LUMO (eV)
C1	1.237	−5.58	381	3.25	−2.33
C2	1.087	−5.43	381	3.25	−2.18
C3	−0.079	−4.26	339	3.66	−0.60
C4	0.878	−5.22	341	3.64	−1.58

HOMO (eV)=− E^{OX} − 4.34 [43, 44], Gap (eV)=1240/λonset, LUMO (eV)=HOMO+gap

Table 5 The change of the dipole moment between the excited state and ground state respectively obtained from experiments and theoretical calculations

Methods	Dipole moments change Δμ (D)			
	C1	**C2**	**C3**	**C4**
From experiment	4.89	3.22		
From theory	3.23	5.06	0.82	3.18

1 D=3.336× 10^{-30} c.m

roles: (1) decreasing the extent of intramolecular charge transfer of **C3** and **C4**; (2) increasing the delocalization of electron density distribution of overall molecule. In other words, the electron density distribution of stilbene part was decreased. The results confirmed that (n, π*) electron transition **C3** and **C4** was considerably inhibited and (π, π*) electron transition of **C1** and **C2** was further strengthened. As a consequence, the absorption of **C3** and **C4** exhibited obvious blue-shift and the fluorescence emission was much reduced. The calculations could well interpret why the absorption and fluorescence wavelength of branched nitro-stilbene derivatives could be efficiently tuned by the chemical linking bond.

We further estimated the changes on the dipole moments between the excited state and ground state based on Lippert equation [45, 46]:

$$hc(\nu_{abs} - \nu_{em}) = \frac{2\left(\mu_e - \mu_g\right)^2}{4\pi\varepsilon_0 a^3}\Delta f + const \tag{4}$$

$$\Delta f = \left(\frac{\varepsilon - 1}{2\varepsilon + 1} - \frac{n^2 - 1}{2n^2 + 1}\right) \tag{5}$$

Wherein h is Planck's constant, c is the speed of light, and Δf is called the orientation polarizability. υ_{abs}, υ_{em} are the wavenumbers of the absorption and emission, n is the refractive index, and ε is the relative low-frequency dielectric constant of the solvents.

Lippert equation, the chromophore group was regarded as a dipole, which located in a cavity with a radius of *a* in a continuous solvent-dipole environment. Moreover, this equation reflected a solvent effect of the index of refraction and relative dielicetric constant. Consequently, the linear correlation between Stokes shifts and Δf could not show some special interaction between the fluorophore and solvent molecules such as hydrogen bonding. Plots of Stokes shift as a function of the solvent orientation polarizability (Δf) was shown in Fig. 9. The linear correlation of **C1** and **C2** between Stokes shift and orientational polarizability suggested the dipolar solvent effects [47, 48]. Two equations were obtained for **C1** and **C2** respectively: **C1**: Y=11855x+5228.5, **C2**: Y=13383x+5070.7. Similar slopes of **C1** and **C2** implied that excited decay processes of **C1** and **C2** were similar [49]. However, the linear correlationship between Stokes shift and orientational polarizability for **C3** and **C4** could not be obtained, suggesting the excited state decay process of **C3** and **C4** was much different from that of **C1** and **C2**. The changes of dipole moments on the excited state and ground state could be calculated from the slopes, and the data were listed in Table 5. Although the experimental and theoretical results had some difference, the data have confirmed simultaneously that **C1** and **C2** had larger charge transfer than **C3** and **C4** in the excited state. In a word, the results suggested that the electron coupling effects induced by excitation delocalization were greatly affected by various linking bonds. Thus, the electron density distribution of chromophore part of **C1** and **C2** was different from **C3** and **C4** in the excited states, which eventually lead to different spectral characteristics.

Thermal analysis

The analysis of the thermal properties was conducted with differential thermal analysis (DTA) and thermogravimetric analysis (TGA) under a nitrogen atmosphere and the results were listed in Fig. 10. The endothermic peaks determined by DTA were found at 170.57, 143.17, 169.59 and 164.77°C for **C1**, **C2**, **C3** and **C4** respectively as presented in Fig. 10. Considering the heating rate was 10°C min^{-1}, the DTA data are very close to the melting points of **C1** to **C4** respectively determined with melting point apparatus. The decomposition temperatures of compounds **1** to **4** determined by TGA were 334.76, 306.62, 359.02 and 376.37°C respectively as shown in Fig. 10. The weight loss of **C1** (MW=313.13) was 37.852% at 334.76°C, which was close to the loss of diethoxy part (MW=87.89). Interestingly, the

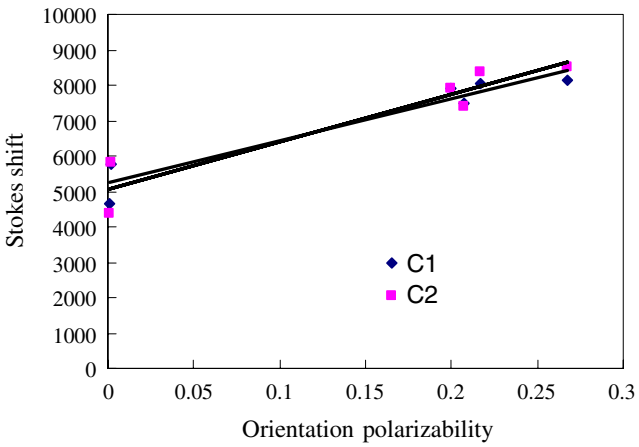

Fig. 8 Electron density distribution of HOMO and LUMO at S_0 and S_1 states

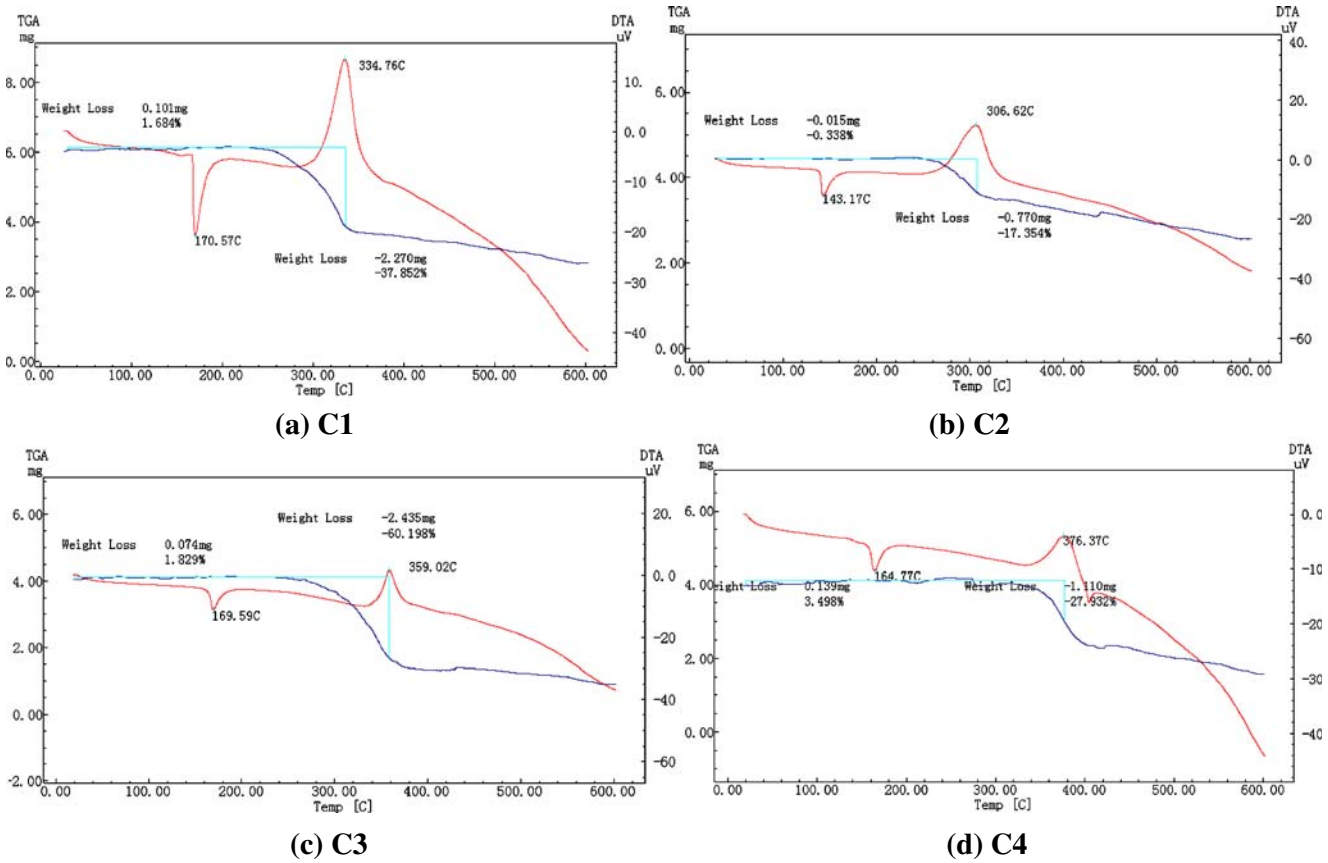

Fig. 9 Relationship between stokes's shifts of **C1** and **C2** and orientation polarizability (Δf) of solvents

weight loss of **C2** (MW=437.16) was 17.354%, which was also close to the loss of benzyl group (MW=76.03). The weight loss of **C3** (MW=341.09) was 60.198%, which was to close to the loss of nitro group and two acetoxy groups (Total: MW=164.10). **C4** (MW=465.12) displayed 27.932% weight loss, which was close to the loss of two benzoyloxy groups (MW=120.02). The analysis showed that: (1) these compounds had remarkable thermal stability and the decomposition temperatures of the compounds **1** to **4** were over 300°C, and (2) intramolecular linking bond did not show large effect on the thermal stabilities.

Conclusions

To summarize, a range of new branched nitro-stilbene derivatives with various linking bonds was synthesized and characterized. The linking bonds showed significant effects on the electron density distribution of HOMO and LUMO, and thus the extent of intramolecular charge transfer exhibited considerably different. This resulted in the different dipole moment changes between the excited state and the ground state for these branched nitro-stilbene derivatives. The results suggested that the ($\pi \rightarrow \pi^*$), ($n \rightarrow \pi^*$) electron transition and the excited state decay process of these compounds were influenced by various chemical bonds. The estimated HOMO and LUMO energies of these compounds revealed further the effects of linking bonds on the electron density distribution of frontier orbital. These made it much possible to tune

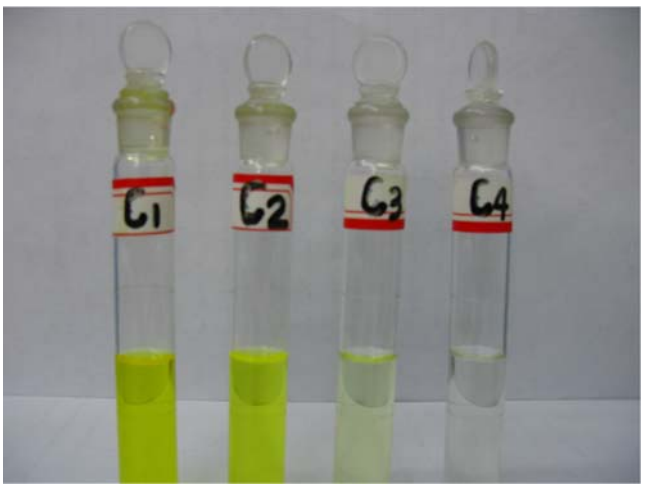

Fig. 10 DTA and TGA curves of the compounds **1** to **4**

efficiently the spectroscopic properties of the branched nitro-stilbene derivatives by linking bond. While, the thermal stabilities of nitro-stilbene derivatives were not afftected by the linking bonds. The results presented in this paper would be great interest in the development various branched substituted nitro-stilbene dyes with required spectroscopic characteristics based on chemical strategy.

Acknowledgements The authors appreciate financial support from the National Natural Science Foundation of China (Nos. 20776165, 20702065, 20872184), Natural Science Foundation of Chongqing Science and Technology Commission (Nos. CSTC 2009BB4216) and the Key Foundation of (CSTC 2008BA4020). H. Li thanks "A Foundation for the Author of National Excellent Doctoral Dissertation of PR China (200735)" for financial support. This paper is part sponsored by the Scientific Research Foundation for the Returned Overseas Chinese Scholars, State Education Ministry as well (Nos. 20071108-1, 20071108-5). L. Yang appreciates support from Chongqing University Postgraduates' Science and Innovation Fund (Nos. 200904A1A0010304).

References

1. Geddes CD, Parfenov A, Roll D, Uddin MJ, Lakowicz JR (2003) Fluorescence spectral properties of indocyanine green on a roughened patinum electrode metal-enhanced. J Fluor 13:453–457
2. Geddes CD, Apperson K, Birch DJS (2000) New fluorescent quinolinium dyes-applications in nanometre particle sizing. Dyes & Pigments 44:69–74
3. Wu X, Chowdhury MH, Geddes CD, Aslan K, Domszy R, Lakowicz JR, Yang AJM (2008) Use of surface plasmon-coupled emission for enhancing light transmission through top-emitting organic light emitting diodes. Thin Solid Films 516:1977–1983
4. Dvornikov AS, Rentzepis PM (1999) Novel organic ROM materials for optical 3D memory devices. Optics Commu. 136:1–6
5. Sun HB, Tanaka T, Takada K, Kawata S (2001) Two-photon photopolymerization and diagnosis of three-dimensional micro-structures containing fluorescent dyes. Appl Phys Lett 79:1411–1413
6. Sayama K, Tsukagoshi S, Hara K, Ohga Y, Shinpou A, Abe Y, Suga S, Arakawa H (2002) Photoelectrochemical properties of J aggregates of benzothiazole merocyanine dyes on a nanostructured TiO_2 film. J Phys Chem B 106:1363–1371
7. Peng X, Song F, Lu E, Wang Y, Zhou W, Fan J, Gao Y (2005) Heptamethine cyanine dyes with a large stokes shift and strong fluorescence: A paradigm for excited-State intramolecular charge transfer. J Am Chem Soc 127(12):4170–4171
8. Hagfeldt A, Gratzel M (2000) Molecular Photovoltaics. Acc Chem Res 33:269–277
9. Hagberg DP, Yum JH, Lee HJ, Angelis FD, Marinado T, Karlsson KM, Humphry-Baker R, Sun L, Hagfeldt A, Gratzel M, Nazeeruddin MK (2008) Molecular engineering of organic sensitizers for dye-sensitized solar cell applications. J Am Chem Soc 130:6259–6266
10. Maus M, Rettig W, Bonafoux D, Lapouyade R (1999) Photoinduced intramolecular charge transfer in a series of differently twisted donor - acceptor biphenyls as revealed by fluorescence. J Phys Chem A 103:3388–3401
11. Hamasaki K, Ikeda H, Nakamura A, Ueno A, Toda F, Suzuki I, Osa T (1993) Fluorescent sensors of molecular recognition. Modified cyclodextrins capable of exhibiting guest-responsive twisted intramolecular charge transfer fluorescence. J Am Chem Soc 115:5035–5040
12. Chen L, Cui Y, Mei X, Qian G, Wang M (2007) Synthesis and characterization of triphenylamino-substituted chromophores for nonlinear optical applications. Dyes & Pigments 72:293–298
13. Jin Z, Xu Q, Li N, Lu J, Xia X, Yan F, Wang L (2008) Facile di-color emission tuning of poly[1-(4-vinylstyryl)naphthalene] with naphthalimide end group via ATRP. Eur Poly J 44:1752–1757
14. Calaminici P, Jug K, Koster AM, Arbez-Gindre C, Screttas CG (2002) Mechanism for large first hyperpolarizabilities of phosphonic acid stilbene derivatives. J Comput Chem 23:291–297
15. Gorman CB, Marder SR (1993) An investigation of the interrelationships between linear and nonlinear polarizabilities and bond-length alternation in conjugated organic molecules. PNAS 90:11297–11301
16. Marder SR, Cheng L, Tiemann BG, Friedli AC (1994) Large first hyperpolarizabilities in push-pull polyenes by tuning of the bond length alternation and aromaticity. Science 5146:511–514
17. Fayed TA, Etaiw SEDH, Khatab HM (2005) Excited state properties and acid-base equilibria of *trans*-2-styrylbenzoxazoles. J Photochem Photobio A: Chem 170:97–103
18. Jha PC, Das M, Ramasesha S (2004) Two-photon absorption cross sections of *trans*-stilbene, and 7, 8-disubstituted stilbenes in different molecular conformations: A model exact study. J Phys Chem 108:6279–6285
19. Lapouyade R, Czeschka K, Majenz W, Rettig W, Gilabert E, Rulliere C (1992) Photophysics of donor-acceptor substituted stilbenes. A time-resolved fluorescence study using selectively bridged dimethylamino cyano model compounds. J Phys Chem 96:9643–9650
20. Perrin DD, Armarego WLF, Perrin DR (1966) Purification of laboratory chemicals. Pergamon, New York
21. Eaton DF (1988) Reference materials for fluorescence measurement. Pure & Appl Chem 60:1107–1114
22. Maus M, Retigg W, Bonafoux D, Lapouyade R (1999) Photoinduced intramolecular charge transfer in a series of differently twisted donor-acceptor biphenyls as revealed by fluorescence. J Phys Chem A 103:3388–3401
23. Lukeman M, Veal D, Wan P, Ranjit V, Munasinghe N, Corrie JET (2004) Photogeneration of 1, 5-naphthoquinone methides via excited-state (formal) intramolecular proton transfer (ESIPT) and photodehydration of 1-naphthol derivatives in aqueous solution. Can J Chem 82:240–253
24. Hyperchem 8.0 Package, Hyperchem Inc., Gainesville, FL
25. Dewar MJS, Zoebisch EG, Healy EF, Stewart JJP (1985) AM1: a new general purpose quantum mechanical molecular model. J Am Chem Soc 107:3902–3909
26. Cavallini G, Massarani E, Process for the preparation of 4-hrdoxystilbene and its derivatives, US Patent 2,878,291
27. Deperasińska I, Dresner J (1998) On the charge-transfer electronic configurations of excited 1, 1′-dinaphthylamine, J. Mol. Stru.: THEOCHEM. THEOCHEM 422:205–212
28. Yang J, He Q, Lin H, Bai F (2001) Probing twisted intramolecular charge transfer state in hyper-branched conjugated polymers. Anal Sci 17:a203–a206
29. Domagalska BW, Wilk KA, Wysocki S (2003) Experimental and theoretical studies on solvent effects of amphiphilic conjugated polyenals. Phys Chem Chem Phys 5:696–702
30. Wang S, Kin S (2009) Photophysical and electrochemical properties of D-π-A type solvatifluochromic isophorone dye for pH molecular switch. Curr Appl Phys 9:783–787
31. Mikroyannidis JA, Stylianakis MM, Cheung KY, Fung MK, Djurisic AB (2009) Alternating phenylenevinylene and thienylenevinylene copolymers with cyano groups: Synthesis, photophysics and photovoltaics. Syn Met 159:142–47

32. Rocha AB, Bielschowsky CE (2001) Intensity of the $n \rightarrow \pi^*$ symmetry-forbidden electronic transition in acetone by direct vibronic coupling mechanism. Chem Phys Lett 337:331–334
33. Roy BC, Gupta MD, Bhowmik L, Ray JK (2001) Synthesis and characterization of poly (2, 5-dimethoxyaniline) and poly (aniline-Co-2, 5- dimethoxyaniline): The processable conducting polymers. Bull Mater Sci 24:389–396
34. Barlow S, Bunting HE, Ringham C, Green JC, Bublitz GU, Boxer SG., Perry JW, Marder SR (1999) Studies of the electronic structures of metallocene-based second-order nonlinear optical dyes. J Am Chem Soc 121:715–3723
35. Li ZM, Wu SK (1996) Study on Photophysical behaviors of styryl pyrazine aerivatives. Acta Phys-Chim Sin 12:418–422
36. Li ZM, Wu SK (1997) The effect of molecular structure on the photophysical behavior of substituted styryl pyrazine derivatives. J Fluor 7:237–242
37. Segura JL, Gomez R, Martin N, Guldi DM (2001) Synthesis of photo- and electroactive stilbenoid dendrimers carrying dibutylamino peripheral groups. Org Lett 3:2645–2648
38. Uda M, Mizutani T, Hayakawa J, Momotake A, Ikegami M, Nagahata R, Arai T (2002) Photoisomerization of stilbene dendrimers: The need for a volume-conserving isomerization mechanism. Photochem & Photobio 76:596–605
39. Squella JA, Sturm JC, Weiss-Lopez B, Bonta M, Nunez-Vergara LJJ (1999) Electrochemical study of β-nitrostyrene derivatives: steric and electronic effects on their electroreduction. J Electroana Chem 466:90–98
40. Ramesh P, Sampath S (2001) Electrochemical and spectroscopic characterization of quinone functionalized exfoliated graphite. Analyst 126:1872–1877
41. Boudon C, Gisselbrecht JP, Gross M, Anthony J, Boldi AM, Faust R, Lange T, Philp D, Van Loon JD, Diederich F (1995) Electrochemical properties of tetraethynylethenes, fully cross-conjugated Π-chromophores, and tetraethynylethene-based carbon-rich molecular rods and dehydroannulenes. J Electroanal Chem 394:187–197
42. Akiyama S, Tajima K, Nakatsuji S, Nakashima K, Abiru K, Watanabe M (1995) Direct C≡C triple bond formation from the C=C Double bond and direct hydroxylation into the o-position of a nitro group on the benzene nucleus with potassium t-butoxide in N, N-dimethylformamide in the air. Bull Chem Soc Japan 68:2043–2051
43. Liu J, Tu G, Zhou Q, Cheng Y, Geng Y, Wang L, Ma D, Jing X, Wang F (2006) Highly efficient green light emitting polyfluorene incorporated with 4-diphenylamino-1,8-naphthalimide as green dopant. J Mat Chem 16:1431–1438
44. Bard AJ, Faulkner LA (1984) Eelctrochemical methods-fundamentals and applications. Wiley, New York
45. Lippert E (1957) Spectroskopische bestimmung des dipolomomentes aromatischer verbindugen im ersten angeregten singulett-zustand. Z. Electrochem. 61:962–975
46. Lakowicz JR (1999) Principles of fluorescence spectroscopy. Kluwer Academic, New York
47. Belfield KD, Bondar MV, Przhonska OV, Schafer KJ (2002) Steady-state spectroscopic and fluorescence lifetime measurements of new two-photon absorbing fluorene derivatives. J Fluor 12:449–454
48. Gaber M, El-Daly SA, Fayed TA (2008) El-Sayed YS Photophysical properties, laser activity and photoreactivity of a heteroaryl chalcone: A model of solvatochromic fluorophore. Optics & Laser Tech 40:528–537
49. Slyadnev MN, Inoue T, Harata A, Ogawa T (2000) A rhodamine and a cyanine dye on the water surface as studied by laser induced fluorescence microscopy, Colloids and Surfaces A: Physicochem. Eng. Asp. Eng. Asp. 164:528–537